# Competition Dynamics between Ancestral Unicellular and Laboratory-Evolved Multicellular *Chlamydomonas reinhardtii*

A Thesis
Presented to
The Academic Faculty

by

Sophia Marin Sukkestad

In Partial Fulfillment
of the Requirements
for Research Option Designation
on the Bachelor of Sciences Degree
in the School of Biological Sciences

Georgia Institute of Technology
April 2020

# Competition Dynamics between Ancestral Unicellular and Laboratory-Evolved Multicellular *Chlamydomonas reinhardtii*

Approved by

Dr. Matthew D. Herron, Faculty Mentor
School of Biological Sciences
*Georgia Institute of Technology*

Dr. Raphael F. Rosenzweig
School of Biological Sciences
*Georgia Institute of Technology*

Dr. Michael D. Goodisman, Undergraduate Research Coordinator
School of Biological Sciences
*Georgia Institute of Technology*

# Table of Contents

# Acknowledgements

I would like to thank Dr. Matthew D. Herron and Dr. Raphael F. Rosenzweig for their continual guidance throughout the writing and experimental process, and for their support throughout my academic and research career. I would also like to thank Dr. Kimberly Chen for her counsel and mentorship during my time with the Volvocine Evolution lab. Lastly, I would like to especially thank my parents and loved ones for their ongoing support throughout my time at the Georgia Institute of Technology and beyond.

# List of Figures and Tables

## Abstract

Life on Earth as humanity comprehends it would be unthinkable without multicellular organisms. Despite the pervasiveness of multicellularity, the mechanisms of its evolutionary origin remain largely a mystery. Fortunately, the advent of experimental evolution has enabled scientists to explore facets of organismal history indiscernible from the fossil record alone. Such studies have successfully facilitated in-lab evolution of multicellular morphs in many species. However, evaluation of selective pressures which increase multicellular fitness remain poorly understood, including whether multicellular organisms are more adept at homeostasis. In this study, I investigated the growth and fitness of undifferentiated *Chlamydomonas reinhardtii* descended from strains evolved under predation selection by Herron *et. al* (2019). These descendant strains were tested for homeostatic efficacy against a unicellular ancestor in a series of competition assays in control and pH-variable media. Overall, I found no significant difference in intrinsic growth rate between multicellular strains and the unicellular competitor in control or acidic mixed cultures. Fitness of all multicellular strains tested, though less than that of the single-celled ancestor, also did not significantly differ when cultivated in acidic versus ideal conditions. These results support previous hypotheses of fitness decrease with increasing body size due to growth constraints, and suggest further investigation into other environmental challenges for longer replicates are necessary.

# Introduction

Multicellular life is found in every biome on Earth. Its diversity of form and function provides a window into the emergence and processes of biological cooperation(1), transitions in individuality(2,3,4), and increasing biological complexity(5). Although multicellular-like organisms first appeared in the fossil record ca. three billion years ago(6), multicellularity has evolved at least twenty-five times in independent eukaryotic lineages(7) across four biological kingdoms(8,9). The prevalence of multicellularity in multiple distinct clades raises questions about why it emerged more than once. Exploring the evolution of this phenotype may provide insight into what selective pressures drive the evolution of higher-order complexity. Such studies can provide a context for the evolution of complex life on Earth as humanity understands it. Also, insights into the evolution of multicellularity are relevant to astrobiology, which aims to investigate the origin, evolution and distribution of life in the universe, and define the conditions required for biocomplexity to undergo 'quantum leaps'(10).

Predation has long been thought to select for multicellularity(11-13), and recent lab evolution experiments support this hypothesis(14). However, it has also been suggested that multicellular structures offer protection from an array of environmental challenges(15-18). For example, the single-celled green alga *Chlamydomonas* spp. can form a transient multicellular structure, the palmella, in response not only to predation, but also to salt-, heat-, and pH-induced stress. This facultative response has been hypothesized to preserve mitotically-produced daughter cells, especially under conditions when mating and zygospore creation may not be possible(19-21). In Volvocine green algae, higher levels of organismal complexity have been correlated with greater survival in environments with low nutrient availability(22). To date however, these correlations have only been made *among* species that differ in their complexity. To rigorously test this hypothesis experiments are required in which stress-resistance is evaluated *within* a single species between forms that are unicellular and those that are multicellular, but that share a recent common ancestor(23).

Wild type *Chlamydomonas reinhardtii* is a haploid unicellular green alga that can grow either as a photoautotroph or a chemoorganotroph(24,25). *C. reinhardtii*'s metabolic versatility, coupled with its ease of laboratory culture, short generation time (~16-24 hr)(26), and capacity for phototaxis, makes it an ideal model organism to study genetics(27,28) and motility(29,30). Important for this study, *C. reinhardtii* is closely related to the multicellular algae in the families Volvocaceae and Goniaceae(3), making this species an excellent target for real-time studies of how simple multicellularity evolves.

Experimental laboratory evolution has the potential to provide raw material for just this type of experiment. And indeed, simple multicellularity has been evolved in multiple species under controlled laboratory conditions(14,31). Evolution of multicellularity by predation selection was recently demonstrated in the green alga *Chlamydomonas reinhardtii*.

Herron *et al*. (2019) established unicellular *C. reinhardtii* founder populations derived by crossing two well-characterized strains (CC-1690 and CC-2290)(32,33). Replicate populations of this ancestor were serially transferred into fresh medium every week for ~750 asexual generations, either in the presence or in the absence of the ciliate *Paramecium tetraurelia*(14). In response to this predation, but not in control settings, heritable multicellularity arose in two replicates that varied by lineage in cell number, body plans, and reproductive strategy. To isolate

the genetic determinants of predation-selected multicellularity, these evolved strains were successively backcrossed with their unicellular ancestor. To test the hypothesis that multicellularity confers a fitness advantage under stress, I subjected mixed cultures of backcrossed multicellular *C. reinhardtii* and their wild-type unicellular ancestor to environmental stress at different intensities.

Freshwater species such as *C. reinhardtii* experience both intermittent and seasonal changes in osmolality, temperature, and pH(34). And it is not unreasonable to suppose that genotype-specific differences in the capacity to adapt to these changes is a determinant of their fitness. Several studies demonstrate high survival efficacy for multicellular organisms when presented with higher metabolic cost(35,36). Investigation of pH variation and its resulting effects on multicellular fitness will demonstrate coexistence and competition dynamics with closely related unicellular counterparts.

The overarching goal of my experiments is to shed light on the costs and benefits of simple, undifferentiated multicellularity by competing multicellular and unicellular *C. reinhardtii* under stress. Specifically, I will test whether multicellular forms are more adept at homeostasis than unicellular forms to which they are closely related. Environmental fluctuation in pH was not a component of the predation experiments from which my multicellular strains were derived. However, if a multicellular descendant grew significantly better than its unicellular ancestor under stress, this would suggest that an increased capacity for homeostasis might help sustain *de novo* multicellularity once it emerges. Confirmation of the adaptive homeostasis hypothesis would underscore its central relevance in the evolution of higher-order complexity(37).

# Literature Review

### *Major evolutionary transitions and the concept of the individual*

John Maynard-Smith and Eörs Szathmáry defined major evolutionary transitions (MET) as changes in biological organization that brought about quantum leaps in biocomplexity(38). The concept of METs is intertwined with the concept of units of selection(39,40), which in turn critically depends on what is meant by an "individual". Evolutionary biologists typically see an "individual" as a Darwinian individual—a member of a population whose members exhibit heritable variation in traits affecting fitness and reproductive success(41). The evolution of multicellular individuals from unicellular Darwinian antecedents was one of the most impactful transitions in individuality to occur in the history of Life, resulting in a change in the unit of selection.

Maynard-Smith and Szathmáry described multiple METs(38). The first transition occurred with the emergence of a cell membrane confining hereditary molecules capable of replicating that membrane and its contents. The second occurred when replicating molecules were organized into chromosomes, which were then integrated with enzymes to store and recreate genetic information. Eukaryogenesis, the third transition in their scheme, was the first partnership of independent genetic units; this likely occurred when an α-Proteobacterium entered into an endosymbiotic relationship with a novel Archaeal lineage. The fourth transition, sexual reproduction (or rather the alternation of generations) required the "invention" of meiosis to produce haploid gametes that undergo syngamy to form a diploid zygote. The fifth transition occurred when multicellular organisms evolved from unicellular ancestors, while the sixth transition, the evolution of eusociality, arose when lineages of "superorganism" arose. These consisted of genetically-related, but non-identical individuals that belong to different roles, only some of which reproduce(42-45).

The fifth transition, the emergence of multicellular individuals from unicellular ones, has fascinated evolutionary biologists for more than a century. The multicellular phenotype is pervasive across multiple lineages (7,46), having evolved once in animals(47) but multiple times in plants(48), fungi(49), and protists(50). Among green algae, and specifically the Viridiplantae, multicellularity has arisen multiple times(51), leading to differences in cell division patterns, adhesion, and differentiation observed among extant groups(9,52). The ecological and genetic factors that favored evolution of multicellularity and sustained it thereafter are incompletely understood, and are subject of investigation in several taxa.

One of these taxa is the biflagellate, haploid alga *Chlamydomonas reinhardtii*. Though single-celled, it is a marginal species of the multicellular Volvocine algae clade. Thus, its outgroup status in the mostly multicellular Volvocine lineage(3) makes it an ideal model in which to investigate the fifth MET: the evolution of multicellular forms from unicellular ancestors. This species may reveal a wealth of information on the pre-requisites of multicellular evolution as it can evolve the multicellular phenotype in the lab under settling rate(53) and predation(14,54) selection. Although this phenomenon has been observed in *C. reinhardtii* and other species (12,31,54), systematic investigations into how specific genetic and environmental factors interplay have only just begun. This is especially true with regard to competition

dynamics between evolutionarily-related unicellular and multicellular forms under abiotic stress. This literature review aims to describe current knowledge about multicellular fitness tradeoffs and the experimental evolution of multicellularity under different types of selection.

***Evolution of simple multicellularity: Selective agents and fitness tradeoffs***

Two mechanisms have been proposed to explain how multicellular organisms might initially arise: (i) aggregation of genetically distinct cells or (ii) continued association of cells that originate from a single clone(55). In the first case, single cells having different genetic origins form a cluster of cells, which in turn produce zygotes or spores that will aggregate once more(6). In the second, daughter cells produced during asexual mitotic division may fail to separate due to an error in cell wall cleavage or an inability to break free of an adhesive exterior, such as an extracellular matrix.

Continued association can be seen in wild-type *Chlamydomonas reinhardtii* during palmelloid formation following mitosis, indicating a degree of phenotypic plasticity for multicellularity. The appearance of palmelloids can occur either when extracellular adhesive secretions in unicellular individuals promote clumping (**Figure 1A**), or by failure of mitotically-produced daughter cells to escape the extracellular matrix (**Figure 1B**)(56). Unicellular *C. reinhardtii* produce palmelloid structures in response to a variety of environmental stressors, ranging from predation(57,58) to fluctuations in environmental salinity and pH to the presence of organic acids such as glutamate(15). Other unicellular organisms can enter a quasi-multicellular state under certain pressures: for example, *Escherichia coli* aggregate under oxidative stress(16). These various determinants of transient multicellularity suggest that unicellular forms sometimes harbor the genetic components necessary for simple multicellularity.

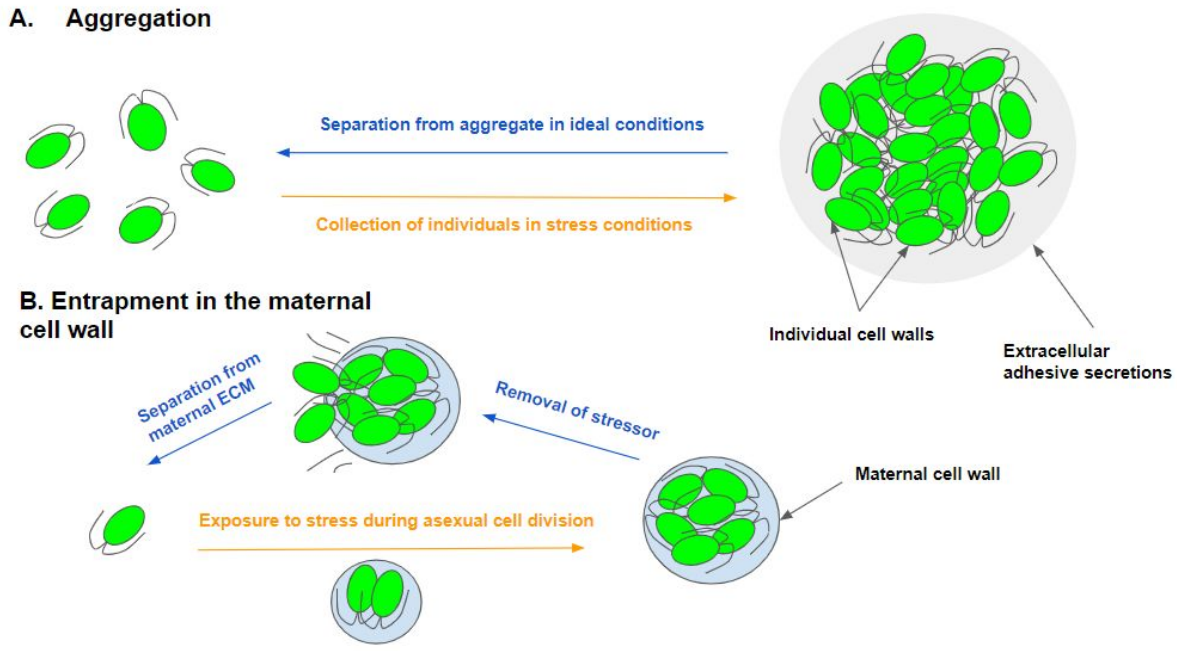


**Figure 1. Formation of palmelloid structures.** *C. reinhardtii* is one of several typically unicellular organisms that can form temporary multicellular clusters to bolster against biotic (predation, other antagonistic behaviors) and abiotic (pH, temperature, salinity extremes) assaults. This can happen via collection of genetically distinct

individuals (A) or failure to separate from the maternal cell wall during mitotic division (B). Both avenues of palmelloid formation can be reversed when the responsible stressor is removed.

Such similarities point to an array of environmental factors to consider when weighing possible selective advantages to multicellularity. Aside from the threat of predation(59,60), a variety of other selective pressures have been proposed that increase fitness of multicellular morphs relative to unicellular forms. Pfeiffer and Bonhoeffer (2003) have conducted simulations which suggest that multicellular structures present opportunities for more diverse metabolic pathways via cooperative production of ATP and digestive secretions(17). Multicellularity may also confer additional benefits in nutrient-limited habitats by increasing an individual's ability to store excess energy(18). If, as these studies suggest, multicellular forms exhibit, relative to their unicellular forms, increased survivorship in the face of environmental challenges, then one benefit of multicellularity might be a greater capacity to maintain homeostasis.

Conversely, the evolution of multicellularity may impose fitness costs to the new individual. Multicellular *C. reinhardtii* experimentally evolved under predation lack motility(14), a trait that is essential for phototaxis. Encasement of flagella in the extracellular matrix, a trait noted in multicellular strains evolved by Herron *et. al* (2019)(61), without cell specialization can exacerbate costs associated with increasing cluster size, particularly with regard to drag and buoyancy(62). Such impairments place limits on cluster size in undifferentiated multicellular body plans(48,63). Slowed somatic growth and longer generation times have also been implicated with increasing cluster size, resulting in lower fecundity(64). Additionally, impediments to photosynthesis via self-shading can arise in non-motile algae having three-dimensional cell arrangement(65,66). Lastly, in aggregative multicellular organisms composed of genetically different cells, the issue of cheating genotypes emerges(67,68). Cheater cells in aggregative clusters reap reproductive benefits from being in the multicellular group inclusion without contributing to the group's energetic demand. Thus, the presence of cheaters can impose both metabolic and reproductive costs on cooperator cells within a mixed group.

In summary, a variety of environmental and genetic factors have the potential to influence the fitness of newly-evolved multicellular forms, relative to their unicellular ancestors, and each of these factors can be evaluated in the laboratory. My experimental design is aimed at understanding how variability in one abiotic factor, extracellular pH, affects survival and reproduction in cells that have recently made the evolutionary transition from single cells to simple, undifferentiated multicellularity.

### *Experimental evolution of multicellularity*

Reconstructing phylogenetic lineages over geologic time benefits from a fossil record corroborated by radiometric dating of that record. However, techniques to reconstruct evolutionary history expand to include those that take into account genomic and paleontological evidence. Experimental evolution makes it possible to directly observe evolution as it occurs, and to infer from those observations how ecology and genetics interplay to generate novel phenotypes(69). In the study of evolutionary complexity, experimental evolution has proven invaluable for elucidating species-specific histories by examining speciation(70), kin selection(71), and influence of environmental variability(72). This method is indispensable in reconstructing the emergence of organisms for which fossil records are tenuous at best, including Volvocine algae(73). Of special relevance to this study, laboratory evolution has been used to

generate multicellular lineages on which genetic, proteomic, and metabolomic analyses may be conducted(reviewed in ref. 69).

Several model organisms have been used to carry out experimental evolution, including the bacterium *Escherichia coli*, the fruit fly *Drosophila melanogaster*, the rotifer *Brachionus calyciflorus*, Baker's yeast *Saccharomyces cerevisiae*, and the green alga *C. reinhardtii*(74-78). Studies such as these have had a variety of aims, ranging from investigations into the evolution of mutation rate(79), the costs and benefits of different levels of ploidy(80), the fate of newly-duplicated genes(81), and the tempo of evolution in the presence(82) and absence(83) of sex, to name but a few. With respect to the evolution of multicellularity, yeast and algal models have proven especially useful. Diverse multicellular morphs of varying cluster size and shape have been observed in *S. cerevisiae* subjected to settling rate selection(84). Additionally, novel multicellular yeast phenotypes grew via adhesion of daughter cells after division from mother cells and reproduced via multicellular propagules(31). Interestingly, increasing settling rate selected for more hydrodynamic morphs that settled more efficiently than ancestors of similar size(85). Settling rate selection was also strongly correlated with apoptotic behavior, demonstrating a tempering of the cluster growth-size tradeoff(31). Similarly, settling rate selection of *C. reinhardtii* produced multicellular morphs that grew via division of daughter cells within the extracellular matrix and reproduced via unicellular propagules(53).

Similar experiments have been conducted in algal species to test the influence of predation on the evolution of multicellularity. When Boraas and colleagues (1998) subjected the alga *Chlorella vulgaris* to protist predation, multicellularity not only became rapidly fixed (<100 generations), but subsequently converged on an optimal cluster size that enabled protection from phagocytosis and adequate nutrient access for individual cells(12). Algal grazing selection has also produced a diverse set of prey life cycles. Heritable palmelloid formation induced by rotifer predation of *C. reinhardtii* was confirmed in as few as nine generations after exposure to *B. calyciflorus*(54). Herron et. al (2019) utilized protist predation over 750 generations to facilitate the evolution of two multicellular populations (B2 and B5) that encompassed strains with three distinct reproductive methods(14).

The use of model organisms such as those described above has substantial merit for evaluating the evolution of organismal complexity. Experiments such as these successfully illustrate for each subject the evolutionary changes incurred, what selective pressures favor their fixation, and how resulting multicellular lineages cope with resulting tradeoffs. Importantly, these resulting multicellular strains exhibit phenotypic stability over many subsequent generations, introducing a potential trove of information to be discovered on their genetics, proteomics, and, with respect to this proposal, competition dynamics.

### *Discussion of Literature*

Several research groups have recently investigated how simple multicellularity can evolve in the lab. These experiments, as well as those analyzing environmental factors that promote palmelloid formation, have shed light on abiotic and biotic factors that favor evolution of multicellularity in the Volvocine algae. To date, however, no one has examined intraspecies interactions between unicellular and multicellular cell types as a way to define the boundary conditions for the evolution of simple multicellularity. Moreover, while a greater capacity for homeostasis has been postulated for multicellular body plans, little is known about the extent of this presumed benefit relative to their unicellular ancestors, and even less is known about underlying causal mechanisms.

To begin to address these knowledge gaps, I will explore the population growth dynamics in lab cultures consisting of either, or both, unicellular and multicellular *C. reinhardtii* under experimental conditions where homeostasis is called into action. The results of this study help to shed light on this stage in the evolution of multicellularity where unicellular and multicellular phenotypes of the same species compete. I have deepened our understanding of whether multicellular body plans are more stress-resistant than unicellular ones because they have greater homeostatic 'buffering capacity', and gained insight into whether de novo multicellularity driven by a biotic factor, predation, can be reinforced by an abiotic factor, the change in extracellular pH.

## Materials and Methods

### *Strains and culture conditions*

Multicellular algal isolates of interest are descended from one of two unicellular *C. reinhardtii* strains and one of two multicellular strains evolved under predation selection in a laboratory setting(14). This was accomplished in two *C. reinhardtii* populations evolved in the presence of the predatory protist *Paramecium tetraurelia* over the course of 750 asexual generations. These two resulting multicellular populations (B2 and B5) have maintained a fixed multicellular phenotype in multiple strains over the course of more than four years on stock agar plates and in liquid media. Strains B2-03 and B5-05 were chosen for backcrossing with unicellular ancestral strains for genetic analysis due to their differences in cluster size and reproductive patterns(14). B5-05 possesses a relatively simple phenotype with an average of four cells per cluster, releasing unicellular propagules during asexual reproduction (**Table 1**). By contrast, the cluster size of B2-03 is much more variable (between 16 and 32 cells/cluster) and releases multicellular propagules during asexual reproduction (**Table 1**). My lab has backcrossed these isolates six times with the wild-type unicellular strain CC-1690(32) over the past year to produce multicellular strains that are isogenic with this unicellular ancestor except for genes responsible for the multicellular phenotype(86). We have successfully isolated multicellular cultures from B2-03xCC-1690 Backcross 6 and B5-05xCC-1690 Backcross (BC) 6.

| *Strain* | *mt* | *Average Cluster Size* | *Asexual Reproductive Strategy* |
|---|---|---|---|
| CC-1690 | + | 1 | 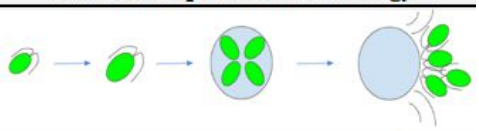 |
| B2-03xCC-1690 BC6: M4 | + | 16-32 | 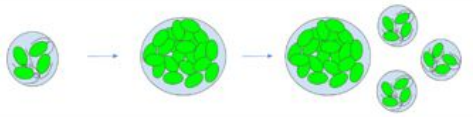 |
| B5-05xCC-1690 BC6: M4 | - | 4 | 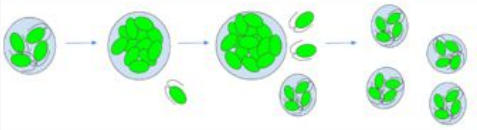 |
| B5-05xCC-1690 BC6: M5 | + | 4 | 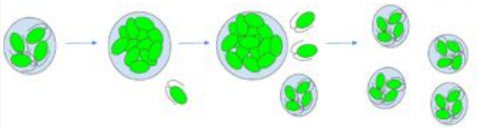 |

**Table 1. List of study strains.** The list shown here details each of the four strains implemented in this study and relevant details regarding their mating type (mt), average cluster size, and asexual reproduction pattern.

### *Backcrossing multicellular strains to produce isolates that genetically differ from their ancestor at one or few loci*

Multicellular strains used in this study were derived from six rounds of backcrossing between isolates from two independently evolved populations (B2-03 and B5-05) from Herron et al (2019)(14) and the + mating type (mt+) unicellular ancestor CC-1690. Original multicellular populations were developed in a laboratory-based evolutionary transfer study that selected for multicellularity under predation as an agent of selection. Successive backcrossing of multicellular isolates to their ancestor produced multicellular strains that had high genetic similarity to that ancestor. These strains are being used in another study to identify genetic mutations that contribute to multicellularity. For this study, backcrossing eliminated genetic variability at other loci that could influence fitness, leaving only variation at multicellular loci. The procedure entailed backcrossing B2-03 and B5-05 (F1 strains of the cross between CC-1690 and CC-2290) with one of the ancestors (CC-1690(mt+)) for six rounds. Over the course of a year, I carried out backcrossing rounds for B2-03 and its multicellular descendants. Backcrossing rounds for B5-05 and subsequent multicellular descendants were conducted chiefly by postdoctoral fellow Dr. Kimberly Chen. Crossings were conducted using a modified protocol from Harris (2009)(56).

***Dynamics of cell growth in experimental monocultures and mixed cultures***

For all competition assays, one multicellular algal strain of each mating type (+ and -) (for B5-05) and one mt+ type (for B2-03) were selected from the BC6 multicellular strains described above. The mt+ ancestor, CC-1690, was chosen as the unicellular competitor in mixed cultures. All five algal strains were separately cultured as "starter monocultures" in 3 mL liquid TAP media (pH~7.00) from 1.5% agar TAP (pH~7.00) stock plates for several days (5-7 days for multicellular strains, 3 days for unicellular strains) until a minimum target density of $10^5$ cells/mL was reached (**Figure 2A**).

On Day 0 of each experiment, starter monoculture densities were determined using a Petroff-Hausser hemocytometer (Hausser Scientific™) and a Zeiss Axiolab light microscope (25x magnification). If starter monoculture densities exceeded $10^7$ cells/mL, they were diluted with liquid TAP (pH~7.00) to a target density of 1-5x$10^6$ cells/mL. Diluted starter monoculture densities were confirmed using a hemocytometer as described above (**Figure 2A**). All hemocytometer counts were conducted by counting the number of colony forming units (CFUs; clusters in multicellular strains, single cells in unicellular strains) rather than counting individual cells to determine total biomass.

Once target density had been achieved, starter monoculture transfer volume necessary for Day 0 monoculture/mixed culture inoculation was calculated based on an experimental initial density of $10^3$ total CFUs/mL in 15 mL liquid TAP (15,000 CFUs/strain/tube in monocultures; 7,500 CFUs/strain/tube in mixed cultures for a 1:1 ratio of unicellular to multicellular CFUs) (**Figure 2A**). Starter monocultures were resuspended, and appropriate volumes were transferred to experimental tubes with 15 mL liquid TAP. To reduce contamination risk during transfer, pipettes and the tops of experimental 15 mL tubes were flamed before transfer, after mixing, and before dilution plating.

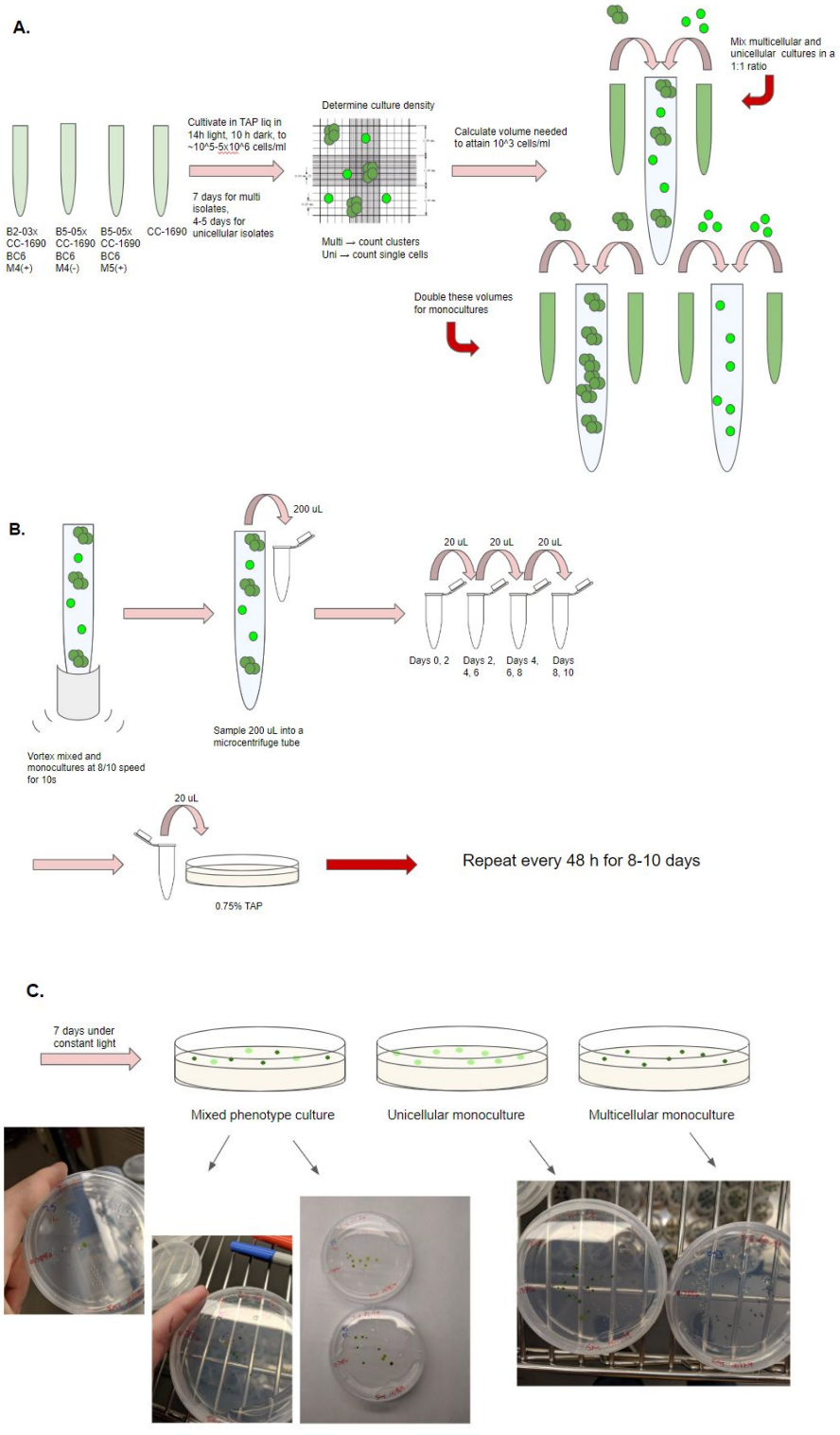


**Figure 2 A-C. General setup for experimental cultures.** The above schematic depicts the process by which (A) starter monocultures are mixed to produce experimental cultures; (B) differential rounds of dilution plating on sampling days; and (C) visual phenotypic variability in unicellular (large, lighter green) and multicellular (small, darker green) colonies.

### *Competition assays*

Control growth curve replicates were carried out in liquid TAP media (pH~7.00) for five monocultures (one unicellular and four multicellular) and four mixed cultures. Differential pH replicates were conducted at pH 5.50, 6.00, 7.00, and 9.00 for five monocultures and pH 5.50, 6.00, and 7.00 for four mixed cultures. Differential pH TAP was created in-house and adjusted for desired pH levels using 1-3N HCl and 1N NaOH. For pH 9.00 liquid TAP, nutrients tended to precipitate and collect on the bottom of stock media bottles after autoclaving. To mediate this, pH 9.00 liquid TAP media was gently shaken and resuspended before inoculation to ensure homogeneous distribution of precipitated nutrients. Cell cultures for the control and different pH treatments were maintained for 8-10 days in a temperature controlled incubator at 22℃ on a 14:10 hour light-dark cycle.

### *Dilution plating*

To determine relative population densities in mixed cultures and monocultures on the day of dilution plating, differentiated colony counts were multiplied by their respective dilution factor and divided in half. For all experiments, mixed cultures and monocultures underwent dilution plating every 48 hours for 8-10 days. Each round of transfer, experimental tubes were rotated to ensure even exposure to incubator light sources. In each round of dilution plating, experimental 15 mL tubes were flamed at the top, inoculated (if transfer occurred on Day 0), and vortexed at 8/10 speed (Vortex-Genie 2, Scientific Industries, Inc.™) for 10 s to ensure homogeneous distribution of cells. Tube tops were flamed once more. 200 µL of culture was transferred to a 1.5 mL microcentrifuge tube and serially diluted with liquid TAP (pH~7.00) tenfold to a total volume of 200 µL for zero to three times depending on the day of transfer in order to reduce overcrowding of agar plates. 20 µL of sample or dilution was then transferred to 0.75% agar TAP plates (pH~7.00) (**Figure 2B**). These plates were stored under constant light at 22℃ for seven days.

After seven days, differential colony counts were conducted based on size to determine the number of multicellular (small, darker colonies) and unicellular (large, lighter green, runny colonies) CFUs in mixed cultures (**Figure 2C**). Colony counts on monoculture plates were not differentiated by size. Colony size difference as a means to identify phenotype was confirmed by microscopic analysis of colonies inoculated in 1 mL TAP in 48-well plates in a preliminary experiment. Mixed cultures were plated as described above and exposed to constant fluorescent light for seven days at 22℃. Once colonies had fully developed, they were transferred to 1 mL TAP in 48-well plates with sections differentiated by colony appearance. Wells were examined by light microscopy to confirm predicted phenotype after 3-4 days of exposure to a 14:10 L:D light cycle at 22-23℃.

Strain-specific densities were calculated for each day of plating by multiplying total differentiated colony counts by the inverse of the corresponding dilution factor and dividing by two. For days with multiple dilution factors, density was calculated using the dilution factor of the plate with total colony counts between 50 and 200 to reduce error from incorrect counting (i.e., counting complicated by an overcrowded plate) or inoculation by chance at low density or high dilution. Total CFU populations were calculated for each day by multiplying strain density by the total culture volume remaining before sampling and plating. Growth curves based on average population CFUs were generated in RStudio. Intrinsic growth rate values *r* were calculated for strains in each replicate by plotting out replicate-specific population curves in Microsoft Excel, fitting an exponential curve with adjusted N(0), and taking the exponential

coefficient. Multicellular fitness values relative to the unicellular ancestor in mixed cultures *W* were calculated for each replicate by dividing the calculated multicellular *r* value by that of the unicellular competitor as described by Lenski *et. al* (1991)(87). The change in multicellular to total population ratio from day 0 to day 8 or 10 was calculated for each replicate by dividing the multicellular population by the total population on both days and subtracting the day 0 ratio from the day 8 or day 10 ratio. All statistical analysis was performed in RStudio.

# Results

### *Control growth curve experiments*

All control growth curve monoculture and mixed culture experiments were conducted over a ten day period. Overall, in ideal growth conditions (pH = 7, 22-23℃) at a 14:10 hour L:D cycle, unicellular ancestor CC-1690(+) in monoculture displays an intermediate increase in density over ten days compared to the four multicellular descendants (**Figure 3**). CC-1690(+) displayed the highest median intrinsic rate of increase *r* behind multicellular B5-05 M5(+), with B5-05 M4(-) and B2-03 M4(+) having the second lowest and lowest median *r* values, respectively (**Figure 4**). However, differences in rate of increase among all strains were not statistically significant (p = 0.08062) in a Kruskal-Wallis H-test comparing median *r* values in ideal condition monocultures (**Table 2**).

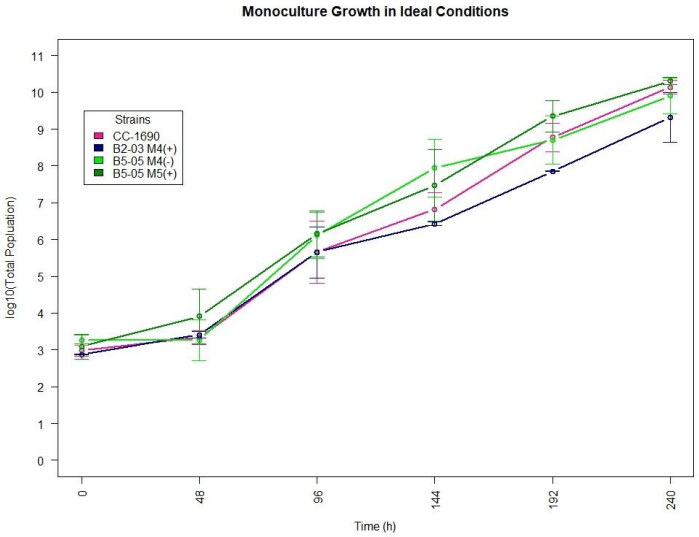


**Figure 3. Average monoculture population in ideal conditions.** The growth curves above display the average monoculture population counts (CFU) over ten days of growth in ideal conditions (pH=7, 22-23℃, 14:10 L:D) for unicellular ancestor CC-1690(+) and four multicellular ancestors from separate lineages. Population calculations were conducted using colony counts on agar plates (0.75%) from the corresponding day multiplied by the plate's dilution factor and total culture volume. Population values are logarithmically scaled. Error bars represent standard deviation for five independent reads per sampling timestamp for CC-1690, B5-05(-), and B5-05(+), and two independent reads per sampling timestamp for B2-03(+).

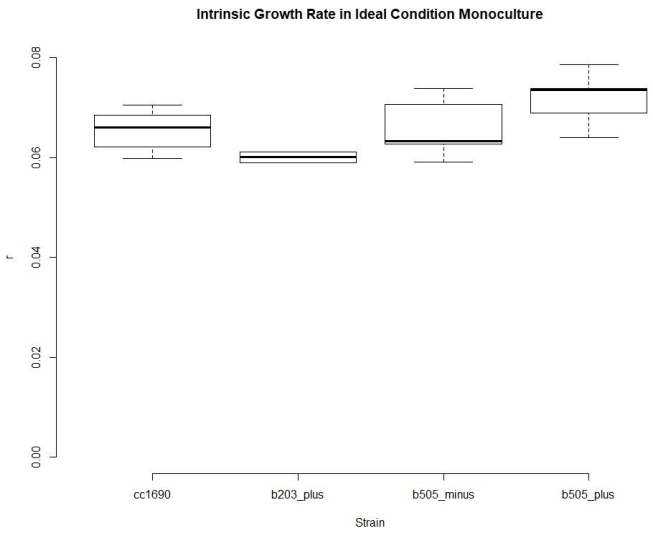


**Figure 4. Distribution of intrinsic growth rate among ideal condition monocultures.** Boxplots above show the spread of intrinsic rate of increase r within monoculture strains in ideal conditions. r values were calculated in Microsoft Excel by fitting an exponential trendline (R^2 > 0.8000) with adjusted intercept (N0) to population growth curves and taking the exponential coefficient.

| *Ideal Condition Monoculture r* | | | | | | | | |
|---|---|---|---|---|---|---|---|---|
| | ***Strain*** | ***Count*** | ***Mean*** | ***SD*** | ***Median*** | ***K-W $\chi^2$*** | ***df*** | ***p-value*** |
| | CC-1690 | 5 | 0.0654 | 0.00443 | 0.0661 | | | |
| | B2-03 + | 2 | 0.0601 | 0.00156 | 0.0601 | | | |
| | B5-05 - | 5 | 0.0659 | 0.00613 | 0.0633 | | | |
| | B5-05 + | 5 | 0.0718 | 0.00553 | 0.0736 | | | |
| | | | | | | *6.7412* | *3* | *0.08062* |
| *Ideal Condition Mixed Culture r* | | | | | | | | |
| | ***Strain*** | ***Count*** | ***Mean*** | ***SD*** | ***Median*** | ***V*** | ***p-value*** | |
| | CC-1690 | 2 | 0.0671 | 0.00113 | 0.0671 | | | |
| | B2-03 + | 2 | 0.0592 | 0.00629 | 0.0592 | *0* | *0.5* | |
| | CC-1690 | 5 | 0.0604 | 0.00906 | 0.0616 | | | |
| | B5-05 - | 5 | 0.0614 | 0.00766 | 0.0593 | *10* | *0.625* | |
| | CC-1690 | 5 | 0.059 | 0.00769 | 0.0603 | | | |
| | B5-05 + | 5 | 0.0611 | 0.00378 | 0.0614 | *8* | *1* | |

**Table 2. Summary statistics: Monoculture and mixed culture intrinsic growth rate.** The table above describes summary statistics of ideal condition monoculture and mixed culture intrinsic growth rates for each strain studied. A Kruskal-Wallis H-test was conducted on median intrinsic *r* values for strains grown in ideal condition monoculture over 10 days. A p-value > 0.05 indicates no significant difference in growth rate among separately cultured strains. Three Wilcoxon Signed Rank tests were conducted to evaluate differences in median intrinsic growth rate between unicellular CC-1690 and a multicellular competitor in ideal condition mixed cultures over 10 days. $p > 0.05$ for all three mixed cultures indicate no significant difference in median *r* between CC-1690 and any of the multicellular competitors.

Average starting ratio of multicellular to total CFUs in mixed culture was confirmed by population calculations based on day 0 colony counts, dilution factor, and culture volume. Mean starting ratios of multicellular to total CFUs ranged from 0.55 (B2-03(+)) (**Figure 5A**) to 0.583 (B5-05(-) and B5-05(+)) (**Figure 5B,C**).

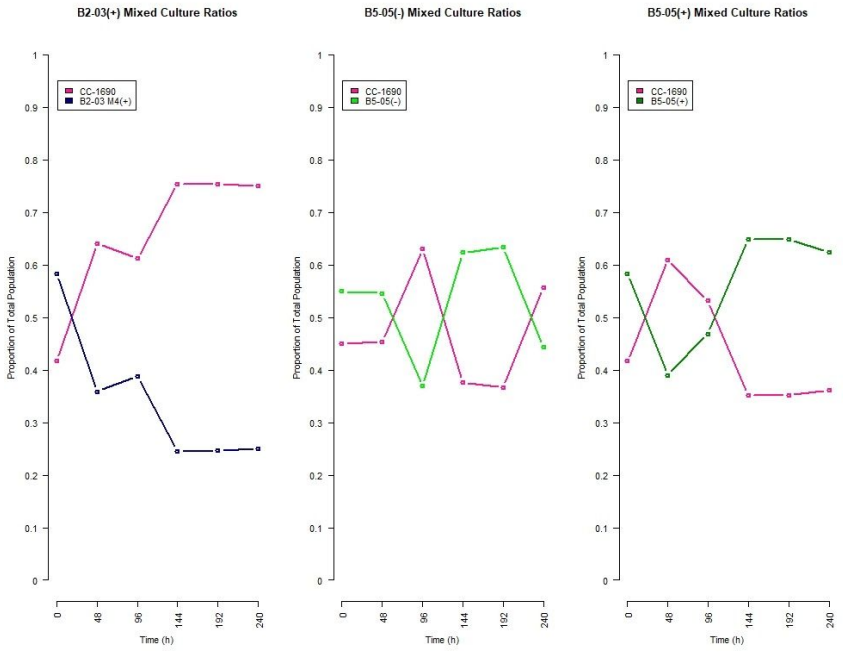


**Figure 5 A-C. Differential strain proportions to total population in ideal condition mixed culture.** The curves above plot the average proportion of CC-1690 and its multicellular competitor strains B2-03(+) (A), B5-05(-) (B), and B5-05(+) (C) per day of sampling in ideal condition mixed culture. Proportions were calculated based on population numbers derived from colony counts, dilution factor, and total culture volume/day. Inoculation volume for each strain was calculated for a theoretical starting proportion of 1:1 unicellular to multicellular CFUs.

In ideal conditions, B2-03 (+) displayed a consistently lower population than CC-1690 in ideal condition mixed culture with the exception of day 0 (**Figure 6A**). B5-05 mt- and mt+ descendants surpassed CC-1690 in variable fashion in ideal condition mixed culture. B5-05(-) population exceeded that of the unicellular ancestor on days 2, 6, and 8, but was surpassed by CC-1690 on day 10 (**Figure 6B**). B5-05(+) population first surpassed that of CC-1690 on day 6 and remained consistently higher in CFU amount than the unicellular competitor through day 10 (**Figure 6C**). Median *r* was higher for CC-1690 against B2-03(+) (**Figure 7A**) and B5-05(-) (**Figure 7B**) and lower against B5-05(+) (**Figure 7C**). Distribution of *r* values ranged widely for B2-03(+) (**Figure 7A**) and B5-05(-) (**Figure 7B**). Three Wilcoxon signed rank tests (**Table 2**) revealed no significant difference in median intrinsic growth rate *r* between CC-1690 and any multicellular strain in mixed culture for B2-03(+) (p=0.50), B5-05(-) (p=0.625), and B5-05(+) (p=1.00) (**Table 2**). Median *r* for the unicellular ancestor decreased in all mixed cultures compared to monocultures with the exception of that with B2-03(+), and all median *r* values for multicellular strains decreased in mixed culture (**Table 2**).

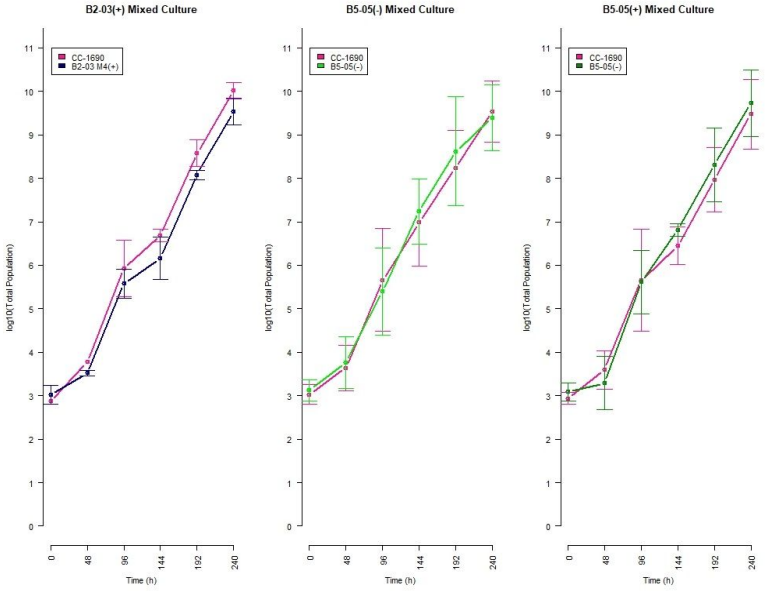


**Figure 6 A-C. Average mixed culture populations in ideal conditions. The growth curves** above show density (CFU/mL) of each B2-03 M4(+) (A), B5-05 M4(-) (B), and B5-05 M5(+) (C) in mixed cultures on each day of sampling over ten days in ideal conditions. Mixed cultures were inoculated at an initial 1:1 7500 CFU/mL ratio. Density calculations were conducted using colony counts on agar plates (0.75%) from the corresponding day multiplied by the plate's dilution factor. Error bars are based on standard deviation for five independent reads per sampling timestamp for B5-05(-) and B5-05(+) mixed cultures, and two independent reads per sampling time stamp for B2-03(+).

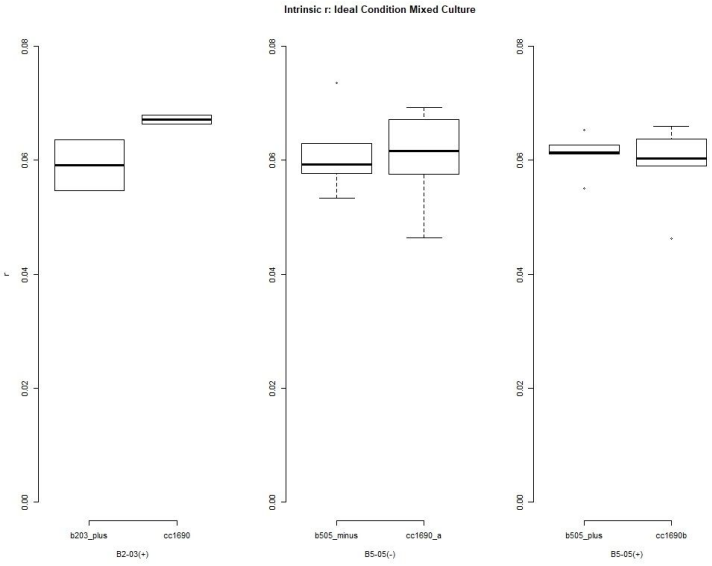


**Figure 7 A-C. Distribution of intrinsic growth rate among ideal condition mixed cultures.** Boxplots above show the spread of intrinsic rate of increase r within mixed culture strains for B2-03(+) (A), B5-05(-) (B), and B5-05(+) (C) in ideal conditions. r values were calculated in Microsoft Excel by fitting an exponential trendline ($R^2 > 0.8000$) with adjusted intercept (N0) to population growth curves and taking the exponential coefficient.

| *pH 6 Monoculture r* | | | | | | | | |
|---|---|---|---|---|---|---|---|---|
| | ***Strain*** | ***Count*** | ***Mean*** | ***SD*** | ***Median*** | ***K-W $\chi^2$*** | ***df*** | ***p-value*** |
| | CC-1690 | 4 | 0.0773 | 0.00863 | 0.0762 | | | |
| | B2-03 + | 3 | 0.0683 | 0.00656 | 0.0679 | | | |
| | B5-05 - | 4 | 0.0643 | 0.00305 | 0.0652 | | | |
| | B5-05 + | 4 | 0.0686 | 0.0103 | 0.0682 | | | |
| | | | | | | *4.5776* | *3* | *0.2055* |
| *pH 7 Monoculture r* | | | | | | | | |
| | ***Strain*** | ***Count*** | ***Mean*** | ***SD*** | ***Median*** | ***W*** | ***p-value*** | |
| | CC-1690 | 4 | 0.0773 | 0.00885 | 0.0807 | *7* | *0.8857* | |
| | B2-03 + | 3 | 0.0751 | 0.00634 | 0.0778 | *1.5* | *0.2683* | |
| | B5-05 - | 4 | 0.0735 | 0.00758 | 0.0758 | *3* | *0.1913* | |
| | B5-05 + | 4 | 0.0671 | 0.012 | 0.0688 | *8* | *1* | |
| *pH 6 Mixed Culture r* | | | | | | | | |
| | ***Strain*** | ***Count*** | ***Mean*** | ***SD*** | ***Median*** | ***V*** | ***p-value*** | |
| | CC-1690 | 3 | 0.0744 | 0.0171 | 0.0776 | | | |
| | B2-03 + | 3 | 0.0641 | 0.0166 | 0.0716 | *0* | *0.25* | |
| | CC-1690 | 4 | 0.0683 | 0.0109 | 0.0668 | | | |
| | B5-05 - | 4 | 0.0662 | 0.00523 | 0.0676 | *3* | *0.625* | |
| | CC-1690 | 4 | 0.0716 | 0.014 | 0.072 | | | |
| | B5-05 + | 4 | 0.0679 | 0.0146 | 0.0688 | *0* | *0.125* | |

**Table 3. Summary statistics: Monoculture and mixed culture intrinsic growth rate in acidic media.** The table above depicts summary statistics for intrinsic growth rate *r* for strains cultured in acidic and neutral media in monoculture and acidic media in mixed culture. A Kruskal-Wallis H-test to analyze the difference in median *r* among CC-1690 and multicellular strains grown at pH =6 in monoculture revealed no significant difference ($p > 0.05$). Pairwise comparisons of median monoculture *r* in neutral and acidic media were not significant ($p > 0.05$) in all four Wilcoxon Rank Sum tests. Three Wilcoxon Signed Rank tests for median *r* of strains pH=6 mixed culture revealed no significant difference between the growth rate of CC-1690 and one of three multicellular competitors ($p > 0.05$).

### *pH-variable growth curve experiments*

Data pertaining to pH 5.50 and 9.00 treatments were excluded from analysis due to inadequate culture growth or complete culture death over the eight day incubation period. The mildly acidic monoculture and mixed culture experiments (pH 6.0) with separate neutral condition controls (pH 7.0) were conducted simultaneously over a period of eight days. In acidic monoculture growth curve experiments (pH = 6.00, 22-23℃) at a 14:10 hour L:D cycle, unicellular CC-1690(+) demonstrated the highest CFU population counts at each timestamp through day 8 except for day 4, at which point B2-03(+) temporarily surpassed the unicellular ancestor (**Figure 8**). B5-05(-) consistently held the lowest monoculture population on each day with the exception of day 8 (**Figure 8**). CC-1690 demonstrated the highest median monoculture *r* compared to all multicellular descendants (**Figure 9**), and experienced a reduction in median intrinsic growth rate from monoculture growth in neutral conditions (**Table 3**). Median *r* decreased for all multicellular strains in acidic monoculture (**Table 3**). A Kruskal-Wallis H-test for differences in median monoculture *r* among strains grown in acidic media revealed no significant difference ($p=0.2055$) in intrinsic growth among strains (**Table 3**). Four Wilcoxon Rank Sum tests demonstrated no significant difference ($p > 0.05$) in median *r* for any strain between acidic and neutral monoculture (**Table 3**).

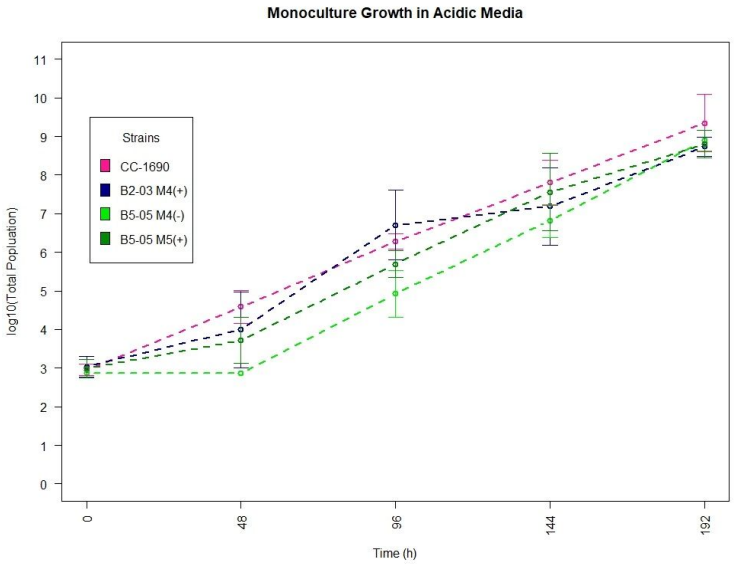


**Figure 8. Average monoculture population in acidic conditions.** The growth curves above display the average monoculture population counts (CFU) over eight days of growth in acidic conditions (pH=6, 22-23℃, 14:10 L:D) for unicellular ancestor CC-1690(+) and four multicellular ancestors from separate lineages. Population calculations were conducted using colony counts on agar plates (0.75%) from the corresponding day multiplied by the plate's dilution factor and total culture volume. Population values are logarithmically scaled. Error bars represent standard deviation for four independent reads per sampling timestamp for CC-1690, B5-05(-), and B5-05(+), and three independent reads per sampling timestamp for B2-03(+). Any average r without error bars had a sample standard deviation of zero.

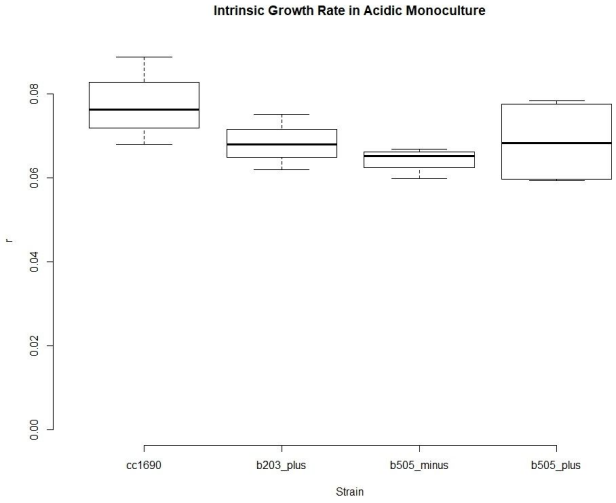


**Figure 9. Distribution of intrinsic growth rate among acidic condition monocultures.** Boxplots above show the spread of intrinsic rate of increase r within monoculture strains in acidic conditions. r values were calculated in Microsoft Excel by fitting an exponential trendline (R^2 > 0.8000) with adjusted intercept (N0) to population growth curves and taking the exponential coefficient.

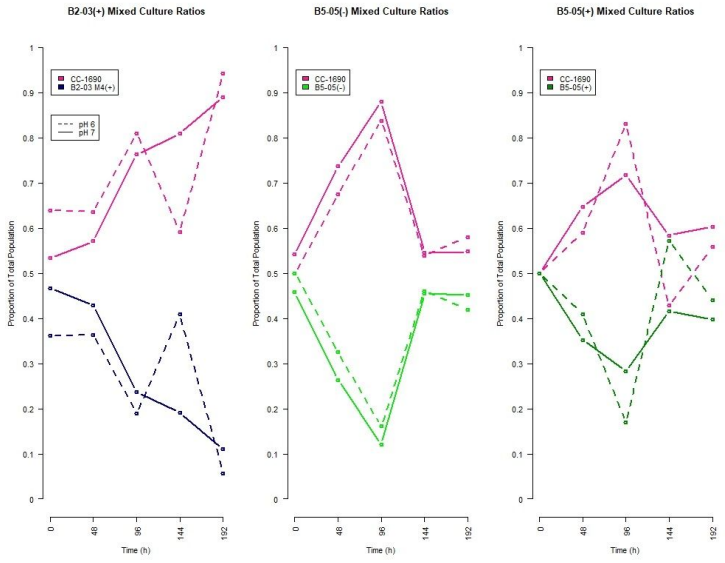


**Figure 10 A-C. Differential strain proportions to total population in acidic and neutral condition mixed culture.** The curves above plot the average proportion of CC-1690 and its multicellular competitor strains B2-03(+) (A), B5-05(-) (B), and B5-05(+) (C) per day of sampling in acidic (dotted line) and neutral (solid line) condition mixed culture. Proportions were calculated based on population numbers derived from colony counts, dilution factor, and total culture volume/day. Inoculation volume for each strain was calculated for a theoretical starting proportion of 1:1 unicellular to multicellular CFUs.

Average starting ratio of multicellular to total CFUs was confirmed as described before. Average starting ratios in mixed cultures ranged from 0.4583 (B5-05(-)) to 0.5 (B5-05(+)) for acidic conditions, and from 0.361 (B2-03(+)) to 0.5 (B5-05(+)) for neutral conditions (**Figure 10 A-C**).

For mixed cultures grown in acidic and neutral conditions, patterns in CFU population growth were variable depending on the specific multicellular competitor. Populations remained steadily higher over eight days in neutral media when compared to acidic conditions for both B2-03(+) and CC-1690, with CC-1690 CFU counts generally superseding those of B2-03(+) in both acidic and neutral media (**Figure 11A**). B5-05(-) mixed culture populations fluctuated more so, with acidic culture populations temporarily surpassing those of neutral cultures for both CC-1690 and B5-05(-) at day 4 only (**Figure 11B**). In general, average population counts for B5-05(-) remained lower than CC-1690 across all eight days of plating in both acidic and neutral media (**Figure 11B**). Similarly, populations in acidic media temporarily exceeded that of neutral media for both B5-05(+) and CC-1690 on days 4 and 6 (**Figure 11C**). Interestingly, population growth of CC-1690 plateaued in neutral media during this interval before returning to typically observed exponential growth (**Figure 11C**). Generally, B5-05(+) populations remained lower than that of the unicellular competitor with the exception of day 6, in which a slight increase over CC-1690 was noted (**Figure 11C**).

In acidic mixed cultures, median intrinsic *r* was higher for CC-1690 than that of the competing multicellular descendant in cultures with B2-03(+) (**Figure 12A**) and B5-05(+) (**Figure 12C**), and lower in culture with B5-05(-) (**Figure 12B**). These median *r* values were lower for all strains in all mixed cultures when compared to neutral media mixed cultures (**Table 3**). Distribution of median *r* was also quite vast for all strains in all acidic mixed cultures (**Figure 12A-C**). Three Wilcoxon Signed Rank tests indicated no significant difference in median intrinsic *r* in acidic medium between the competing unicellular ancestor and B2-03(+) (p=0.25), B5-05(-) (p=0.625), or B5-05(+) (p=0.125) (**Table 3**).

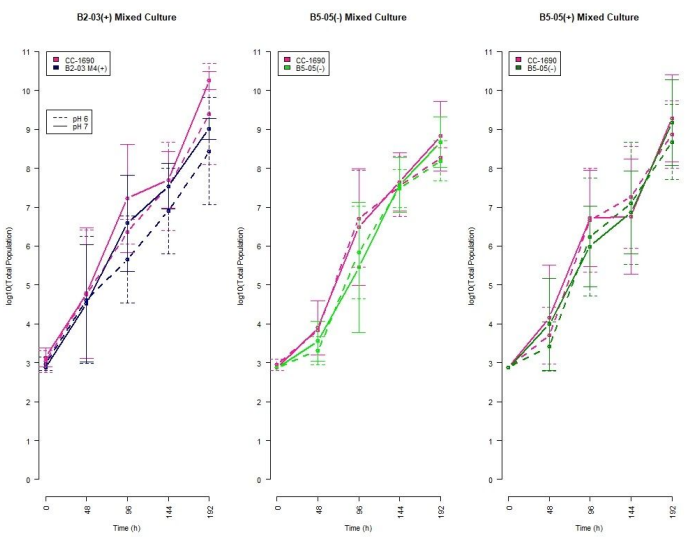


**Figure 11 A-C. Average mixed culture populations in acidic versus neutral conditions.** The growth curves above show population (CFU) of each B2-03 M4(+) (A), B5-05 M4(-) (B), and B5-05 M5(+) (C) in mixed cultures on each day of sampling over eight days in neutral conditions. Mixed cultures were inoculated at an initial 1:1 7500 CFU/mL ratio. Population calculations were conducted using colony counts on agar plates (0.75%) from the corresponding day multiplied by the plate's dilution factor and the total culture volume. Population values are logarithmically scaled. Error bars are based on standard deviation for four independent reads per sampling timestamp for B5-05(-) and B5-05(+) mixed cultures, and three independent reads per sampling time stamp for B2-03(+).

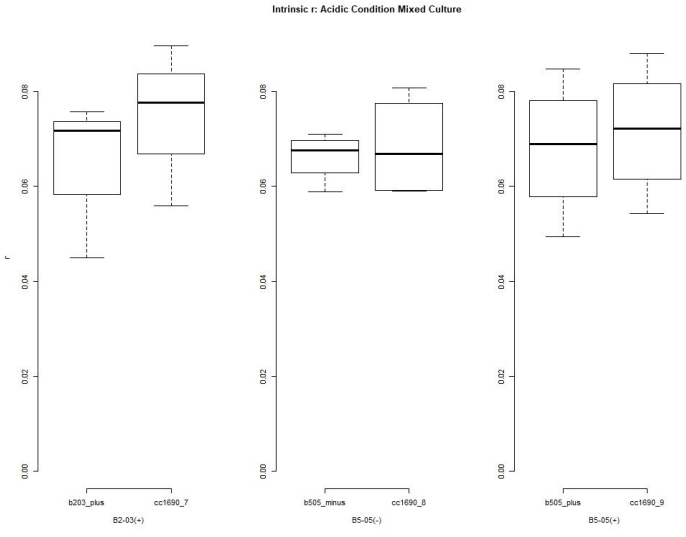


**Figure 12 A-C. Distribution of intrinsic growth rate among acidic condition mixed cultures.** Boxplots above show the spread of intrinsic rate of increase r within mixed culture strains for B2-03(+) (A), B5-05(-) (B), and B5-05(+) (C) in acidic conditions. r values were calculated in Microsoft Excel by fitting an exponential trendline ($R^2 > 0.8000$) with adjusted intercept (N0) to population growth curves and taking the exponential coefficient.

Difference in multicellular fitness relative to the unicellular ancestor (*W*) between acidic and neutral conditions varied among multicellular strains. Median *W* was markedly higher in neutral media for B2-03(+) (**Figure 13A**) and somewhat higher in neutral media for B5-05(+) (**Figure 13C**). The opposite was observed for B5-05(-), which demonstrated a slightly elevated *W* in acidic media (**Figure 13B**). Distribution of *W* values tended to range more vastly for multicellular strains grown in acidic media for B2-03(+) (**Figure 13A**) and B5-05(-) (**Figure 13B**) and in neutral media for B5-05(+) (**Figure 13C**). Three Wilcoxon Rank Sum tests revealed no significant difference in median *W* between acidic and neutral conditions for B2-03(+) (p=0.2), B5-05(-) (p=1.00), and B5-05(+) (p=0.3429) (**Table 4**).

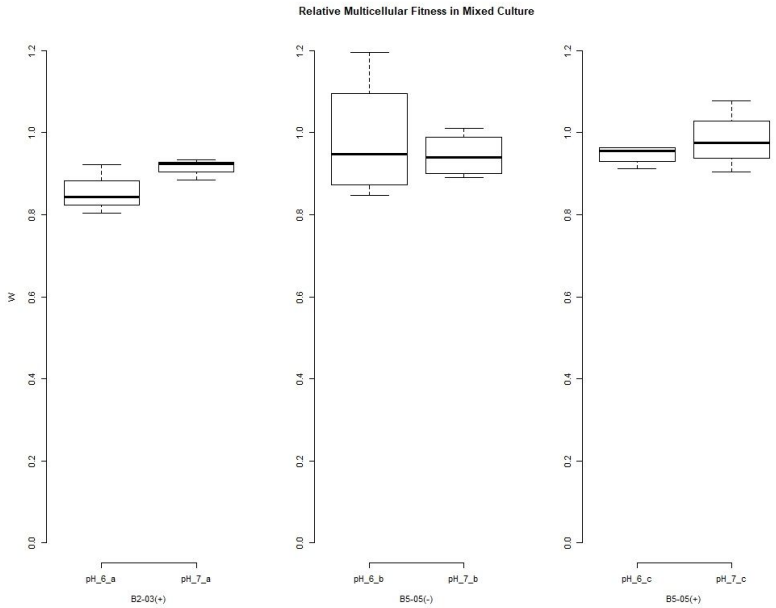


**Figure 13 A-C. Distribution of relative multicellular fitness among acidic and neutral condition mixed cultures.** Boxplots above show the spread of multicellular fitness relative to CC-1690 *W* within mixed culture strains for B2-03(+) (A), B5-05(-) (B), and B5-05(+) (C) in acidic and neutral conditions. *W* values were calculated in Microsoft Excel by dividing intrinsic *r* for multicellular strains by that of CC-1690 for each mixed culture replicate.

| ***pH 6 Mixed Culture W*** | | | | | | | |
|---|---|---|---|---|---|---|---|
| | ***Strain*** | ***Count*** | ***Mean*** | ***SD*** | ***Median*** | | |
| | B2-03 + | 3 | 0.857 | 0.06 | 0.844 | | |
| | B5-05 - | 4 | 0.985 | 0.154 | 0.948 | | |
| | B5-05 + | 4 | 0.946 | 0.0243 | 0.955 | | |
| ***pH 7 Mixed Culture W*** | | | | | | | |
| | ***Strain*** | ***Count*** | ***Mean*** | ***SD*** | ***Median*** | ***W*** | ***p-value*** |
| | B2-03 + | 3 | 0.914 | 0.0262 | 0.924 | *1* | *0.2* |
| | B5-05 - | 4 | 0.945 | 0.0547 | 0.939 | *8* | *1* |
| | B5-05 + | 4 | 0.983 | 0.0712 | 0.976 | *4* | *0.3429* |

**Table 4. Summary statistics: Relative multicellular fitness among acidic and neutral mixed cultures.** The table above shows summary statistics for multicellular fitness relative to CC-1690 *W* in acidic and neutral media for all multicellular strains. Three Wilcoxon Rank Sum tests revealed no significant difference (p>0.05) in median fitness relative to the unicellular ancestor between acidic and neutral mixed cultures for any multicellular strain.

Difference in change of multicellular population to total population ratio from day 0 to day 8 (Δ ratio) between acidic and neutral conditions likewise varied among multicellular strains. Median Δ ratio followed the similar pattern as median *W* values, with markedly reduced reductions for B2-03(+) (**Figure 14A**), slightly increased reductions for B5-05(-) (**Figure 14B**), and slightly decreased reductions for B5-05(+) (**Figure 14C**) in neutral media. Distributions likewise varied vastly with the exception of B5-05(-) in neutral media (**Figure 14B**). Three Wilcoxon Rank Sum tests revealed no significant difference in median Δ ratio between acidic and neutral conditions for B2-03(+) (p=1.00), B5-05(-) (p=0.8857), and B5-05(+) (p=0.8857) (**Table 5**).

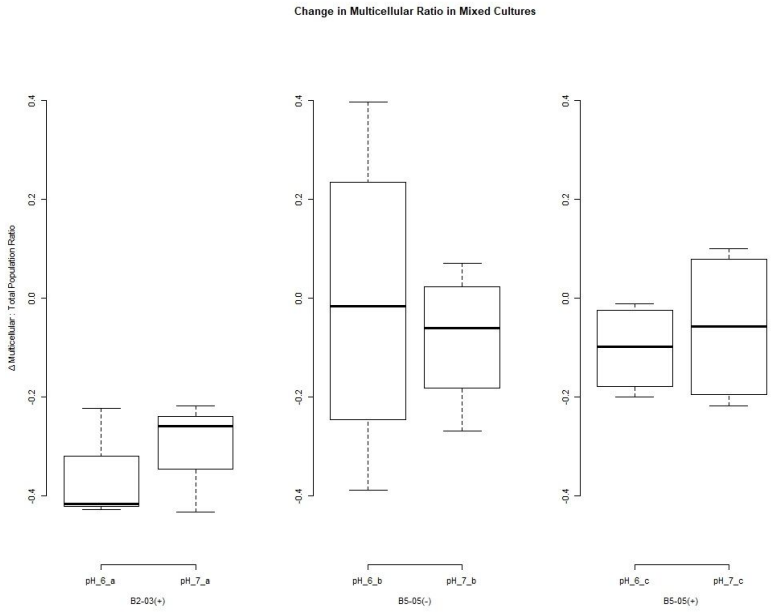


**Figure 14 A-C. Distribution of change in multicellular to total population ratio among acidic and neutral condition mixed cultures.** Boxplots above show the spread of change in multicellular to total population ratio from day 0 to day 8 (Δ ratio) within mixed culture strains for B2-03(+) (A), B5-05(-) (B), and B5-05(+) (C) in acidic and neutral conditions. Δ ratio values were calculated in Microsoft Excel by subtracting day 8 multicellular to total population ratio from that of day 0 for each mixed culture replicate.

| ***pH 6 Mixed Culture Δ ratio*** | | | | | | | |
|---|---|---|---|---|---|---|---|
| | ***Strain*** | ***Count*** | ***Mean*** | ***SD*** | ***Median*** | | |
| | B2-03 + | 3 | -0.356 | 0.115 | -0.417 | | |
| | B5-05 - | 4 | -0.0064 | 0.328 | -0.0162 | | |
| | B5-05 + | 4 | -0.103 | 0.0912 | -0.0992 | | |
| ***pH 7 Mixed Culture Δ ratio*** | | | | | | | |
| | ***Strain*** | ***Count*** | ***Mean*** | ***SD*** | ***Median*** | ***W*** | ***p-value*** |
| | B2-03 + | 3 | -0.304 | 0.114 | -0.26 | *4* | *1* |
| | B5-05 - | 4 | -0.0805 | 0.143 | -0.0611 | *9* | *0.8857* |
| | B5-05 + | 4 | -0.0591 | 0.16 | -0.0588 | *7* | *0.8857* |

**Table 5. Summary statistics: Change in multicellular to total population ratio.** The table above depicts summary statistics for the change in multicellular to total population ratio from day 0 to day 8 (Δ ratio). Three Wilcoxon Rank Sum tests revealed no significant difference ($p > 0.05$) in median Δ ratio for any multicellular strain in acidic versus neutral mixed culture.

## Discussion

Upon examination of control growth data in ideal conditions, several findings can be clearly interpreted. The first of these involves the decrease in intrinsic *r* for all strains when cultivated in a mixed culture versus a uniform monoculture. This logically fits with the ecological principles that the presence of competitors in any fashion decreases resource availability. Intraspecific exploitative competition in this case between the unicellular ancestor and multicellular descendant would account for this decrease when compared to separate cultivation of strains, in which strains must only compete with themselves for nitrogen- and potassium-based nutrients and for space. Given our strains continued with an exponential growth pattern up to the final day of plating, future experiments extending beyond ten days may successfully demonstrate a carrying capacity for both unicellular and multicellular strains in ideal conditions.

Additionally, the lack of significant difference in intrinsic *r* between the unicellular ancestor and all multicellular descendants in ideal condition monoculture may indicate minimal cost to reproductive fitness is incurred by a simple, undifferentiated multicellular body plan. This is confirmed by multicellular fitness values that, while not equal to 1, approach the threshold for equal fitness to the unicellular competitor in both acidic and neutral environments. Though previous work has clearly demonstrated marked decreases in fitness in this respect for differentiated organisms with soma(88), evolutionary mathematical models suggest there is no substantial fitness detriment for undifferentiated multicellular organisms with sizes of four cells or less(89). This explains the phenomenon of the B2-03 descendant possessing the lowest fitness relative to the ancestor, given its larger body size (n=32 cells) when compared with B5-05 descendants (n=4 cells).

Though this fitness cost is minimal, it should be noted that our multicellular strains are still not equally as fit as the unicellular competitor. This logically follows given models that suggest cells must act synergistically in a multicellular cluster in order for multicellularity to evolve as a stable phenotype(89). Such a concept applies in this case: since the original selective pressure under which multicellular ancestors of our strains evolved (i.e., predation), and thereby removing the original benefit incurred, the multicellular body plan may incur fitness cost in comparison. In this instance, this would reveal that slightly acidic conditions would not constitute a substantial environmental stressor for our multicellular strains enough to increase fitness, given the absence of significant difference in intrinsic *r* for multicellular strains in acidic and neutral mixed cultures.

This circumstance of trivial stress imposed by slight acidity may be explained by the lack of dissolved heavy metals typically associated with acidic environments in nature. While *C. reinhardtii*'s limits in pH are well-established, and high cell wall affinity for metallic cations is known(90), acidic media implemented in this study lacked integration of dissolved heavy metals such as Zn, Fe, Cd, Ni, and Pb known to make acidic environmental traditionally detrimental for mesophilic organisms(35). Implementing these heavy metals into liquid TAP media adjusted with 1M HCl in future competition experiments may shed light on multicellular efficacy in this respect, particularly considering the additional safeguard of the ECM and shielding of internal body cells in our multicellular strains.

## Future Directions

Given intrinsic rates of increase are not significantly different from that exhibited by the unicellular ancestor, and given the same holds true for multicellular fitness and change in population ratio between acidic and neutral conditions, several paths for future experiments will be necessary for clarifying the influence of abiotic factors on multicellular evolution. The lack of substantial difference for acidic monocultures and mixed cultures may suggest a need for more extreme pH values in either direction. Additionally, variable measures of error and wide spread of data in some sets may necessitate different methods of data collection, such as increasing the sample size, or strain-specific fluorescent tagging when the genomes of multicellular descendants are more clarified. Extending the length of data collection beyond 8-10 days and increasing the frequency of data collection per replicate may also serve to elucidate growth trends in high density that went beyond the scope of this study.

Exploration of differential survival under heat shock conditions by plating and flow cytometry will also serve as a useful tool to measure multicellular body plan efficacy against the ancestor in the face of common environmental insults. Prolonged exposure to adjusted temperatures in either direction from the ideal (22℃) and cold shock are also possible routes for discovery. The perhaps most interesting abiotic factor that has yet to be examined is variable light stress and the influence of phototaxis in Chlorophyte multicellular fitness and metabolism. Lastly, examining the interplay of other biotic effects, such as interspecies competition, mutualism, and general non-predatory antagonism, will be key to understanding the full context of multicellular emergence from an ecological and evolutionary perspective.

## References


1. Gulli, J. G., Herron, M. D. & Ratcliff, W. C. Evolution of altruistic cooperation among nascent multicellular organisms. *Evolution* **73,** 1012–1024 (2019).
2. Ratcliff, W. C., Herron, M., Conlin, P. L. & Libby, E. Nascent life cycles and the emergence of higher-level individuality. *Philosophical Transactions of the Royal Society B: Biological Sciences* **372,** 20160420 (2017).
3. Herron, M. D. & Nedelcu, A. M. Volvocine Algae: From Simple to Complex Multicellularity. *Evolutionary Transitions to Multicellular Life: Principles and Mechanisms* 129–152 (2015).
4. West, S. A., Fisher, R. M., Gardner, A. & Kiers, E. T. Major evolutionary transitions in individuality. *PNAS* **112**(33): 10112–10119 (2015).
5. Herron, M. D. Fitness and Individuality in Complex Life Cycles. *Philosophy of Science* **83,** 828–834 (2016).
6. Grosberg, R. K. & Strathmann, R. R. The Evolution of Multicellularity: A Minor Major Transition? *Annual Review of Ecology, Evolution, and Systematics* **38,** 621–654 (2007).
7. Parfrey, L. W. & Lahr, D. J. G. Multicellularity arose several times in the evolution of eukaryotes (Response to DOI 10.1002/bies.201100187). *BioEssays* **35,** 339–347 (2013).
8. Niklas, K. J. The evolutionary-developmental origins of multicellularity. *American Journal of Botany* **101,** 6–25 (2013).
9. Bonner, J. T. The origins of multicellularity. *Integrative Biology: Issues, News, and Reviews* **1,** 27–36 (1998).
10. Astrobiology Strategy. *Astrobiology at NASA: Life in the Universe* Available at: https://astrobiology.nasa.gov/research/astrobiology-at-nasa/astrobiology-strategy/. (Accessed: 5th December 2019)
11. Buss, L. W. The Evolution of Individuality. (1988). doi:10.1515/9781400858712
12. Boraas, M. E., Seale, D. B. & Boxhorn, J. E. Phagotrophy by a flagellate selects for colonial prey: A possible origin of multicellularity. *Evolutionary Ecology* **12,** 153–164 (1998).
13. Pentz, J. T., Limberg, T., Beermann, N. & Ratcliff, W. C. Predator Escape: An Ecologically Realistic Scenario for the Evolutionary Origins of Multicellularity. *Evolution: Education and Outreach* **8,** (2015).
14. Herron, M. D. *et al*. De novo origins of multicellularity in response to predation. *Nature: Scientific Reports* **9**:2328 (2019).
15. Iwasa, K. & Mukakami, S. Palmelloid formation of *Chlamydomonas* I. Palmelloid formation by organic acids. *Physiol. Plant.* **21**, 1224–1233 (1968).
16. Ma, M. & Eaton, J. W. Multicellular oxidant defense in unicellular organisms. *Proceedings of the National Academy of Sciences* **89,** 7924–7928 (1992).
17. Pfeiffer, T. & Bonhoeffer, S. An evolutionary scenario for the transition to undifferentiated multicellularity. *Proceedings of the National Academy of Sciences* **100,** 1095–1098 (2003).

18. Szathmary E, Wolpert L. The transition from single cells to multicellularity. ´ See Hammerstein 285–304 (2003).
19. A. Coleman The Roles of Resting Spores and Akinetes in Chlorophyte Survival Cambridge University Press (1983).
20. Visviki, I. & Santikul, D. The pH Tolerance of Chlamydomonas applanata (Volvocales, Chlorophyta). *Archives of Environmental Contamination and Toxicology* **38**, 147–151 (2000).
21. Khona, D. K. et al. Characterization of salt stress-induced palmelloids in the green alga, Chlamydomonas reinhardtii. *Algal Research* **16**, 434–448 (2016).
22. Rokas, A. The molecular origins of multicellular transitions. *Current Opinion in Genetics & Development* **18**, 472–478 (2008).
23. Pentz, Jennifer T, et al. Ecological Advantages and Evolutionary Limitations of Aggregative Multicellular Development. *BioRxiv* (2018).
24. Levine, R. P. The Analysis of Photosynthesis Using Mutant Strains of Algae and Higher Plants. *Annual Review of Plant Physiology* **20,** 523–540 (1969).
25. Sasso, S., Stibor, H., Mittag, M. & Grossman, A. R. From molecular manipulation of domesticated *Chlamydomonas reinhardtii* to survival in nature. *eLife* **7,** (2018).
26. Harris, E. H. *Chlamydomonas* as a model organism. *Annual Review of Plant Physiology and Plant Molecular Biology* **52**, 363–406 (2001).
27. Remacle, C., Cardol, P., Coosemans, N., Gaisne, M. & Bonnefoy, N. High-efficiency biolistic transformation of Chlamydomonas mitochondria can be used to insert mutations in complex I genes. *Proceedings of the National Academy of Sciences* **103,** 4771–4776 (2006).
28. Merchant, S. S. *et. al* The *Chlamydomonas* genome reveals the evolution of key animal and plant functions. *Science* **318**:245–251 (2007).
29. Goodenough, U. W. Substructure of inner dynein arms, radial spokes, and the central pair/projection complex of cilia and flagella. *The Journal of Cell Biology* **100,** 2008–2018 (1985).
30. Nicastro, D. *et. al* The molecular architecture of axonemes revealed by cryoelectron tomography. *Science* **313**, 944–948 (2006).
31. Ratcliff, W. C., *et. al* Experimental Evolution of Multicellularity. *Proceedings of the National Academy of Sciences* **109**, 1595–1600 (2012).
32. CC-1690 wild type mt [Sager 21 gr]. *Chlamydomonas Resource Center* Available at: https://www.chlamycollection.org/product/cc-1690-wild-type-mt-sager-21-gr/. (Accessed: 27th September 2019).
33. CC-2290 S1 D2 mt. *Chlamydomonas Resource Center* Available at: https://www.chlamycollection.org/product/cc-2290-s1-d2-mt/. (Accessed: 27th September 2019).

34. Min, S. K., Yoon, G. H., Joo, J. H., Sim, S. J. & Shin, H. S. Mechanosensitive physiology of chlamydomonas reinhardtii under direct membrane distortion. *Scientific Reports* **4,** (2014).
35. Messerli, M. A. *et al*. Life at acidic pH imposes an increased energetic cost for a eukaryotic acidophile. *Journal of Experimental Biology* **208,** 2569–2579 (2005).
36. Fan, J., Zheng, L., Bai, Y., Saroussi, S. & Grossman, A. R. Flocculation of *Chlamydomonas reinhardtii* with different phenotypic traits by metal cations and high pH. *Frontiers in Plant Science* **8,** (2017).
37. Gould, S. The spandrels of San Marco and the Panglossian paradigm: a critique of the adaptationist programme. *Proceedings of the Royal Society of London. Series B. Biological Sciences* **205**, 581–598 (1979).
38. Smith, J. M. & Szathmary, E. The Major Transitions of Evolution. *Nature* **374,** 227–232 (1995).
39. Michod, R. E. & Roze, D. Cooperation and conflict in the evolution of multicellularity. *Heredity* **86,** 1–7 (2001).
40. Okasha, S. Multilevel Selection and the Major Transitions in Evolution. *Philosophy of Science* **72,** 1013–1025 (2005).
41. Lloyd, E. A. and Gould, S .J. Individuality and adaptation across levels of selection: how shall we name and generalize the unit of Darwinism? *Proceedings of the National Academy of Sciences USA* **96**, 11904–11909 (1999).
42. Emerson, A. E. Social Coordination and the Superorganism. *American Midland Naturalist* **21,** 182 (1939).
43. Wilson, D. S. & Sober, E. Reviving the superorganism. *Journal of Theoretical Biology* **136,** 337–356 (1989).
44. Reeve, H. K. & Holldobler, B. The emergence of a superorganism through intergroup competition. *Proceedings of the National Academy of Sciences* **104,** 9736–9740 (2007).
45. Gardner, A. & Grafen, A. Capturing the superorganism: a formal theory of group adaptation. *Journal of Evolutionary Biology* **22,** 659–671 (2009).
46. Kaiser, D. Building a Multicellular Organism. *Annual Review of Genetics* **35,** 103–123 (2001).
47. King, N. The Unicellular Ancestry of Animal Development. *Developmental Cell* **7,** 313–325 (2004).
48. Kirk, D. L. *Volvox: molecular-genetic origins of multicellularity and cellular differentiation*. (Cambridge University Press, 1998).
49. Medina M, Collins A, Taylor J, Valentine JW, Lipps J, et al. Phylogeny of Opisthokonta and the evolution of multicellularity and complexity in Fungi and Metazoa. *Int. J. Astrobiol*. **2**, 203–211 (2003).
50. Hagen, J. B. Five Kingdoms, More or Less: Robert Whittaker and the Broad Classification of Organisms. *BioScience* **62,** 67–74 (2012).
51. Niklas, K. J. & Newman, S. A. The origins of multicellular organisms. *Evolution & Development* **15**, 41–52 (2013).
52. Kirk, D. L. A twelve-step program for evolving multicellularity and a division of labor. *BioEssays* **27**, 299–310 (2005).

53. Ratcliff, W. C. *et al.* Experimental evolution of an alternating uni- and multicellular life cycle in *Chlamydomonas reinhardtii*. *Nature Communications* **4**: 2742**,** (2013).
54. Becks, L., Ellner, S. P., Jones, L. E. & Hairston, N. G. Reduction of adaptive genetic diversity radically alters eco-evolutionary community dynamics. *Ecol. Lett.* **13**, 989–997 (2010).
55. Tarnita, C. E., Taubes, C. H. & Nowak, M. A. Evolutionary construction by staying together and coming together. *Journal of Theoretical Biology* **320,** 10–22 (2013).
56. Harris, E. H. *The Chlamydomonas Sourcebook*, *Second Edition*. (Academic Press, 2009).
57. Mikheeva, T. & Kruchkova, H. Morphological changes in *Chlamydomonas* sp. and *Scenedesmus acuminatus* in the presence of zooplankton. *Botanica* **5**, 60–63 (1980).
58. Lurling, M. & Beekman, W. Palmelloids formation in *Chlamydomonas reinhardtii*: defence against rotifer predators? *Ann. Limnol. - Int. J. Limnol.* **42**, 65–72 (2006).
59. Stanley, S. M. An Ecological Theory for the Sudden Origin of Multicellular Life in the Late Precambrian. *Proceedings of the National Academy of Sciences* **70,** 1486–1489 (1973).
60. Bell G. The origin and early evolution of germ cells as illustrated in the Volvocales. In *The Origin and Evolution of Sex*, ed. H Halvorson, A Monroy, 221–56. (1985).
61. Boyd M., Rosenzweig F., Herron M. D. Analysis of motility in multicellular *Chlamydomonas reinhardtii* evolved under predation. *PLoS ONE* **13**(1): e0192184. (2018).
62. Solari, Kessler & Michod. A Hydrodynamics Approach to the Evolution of Multicellularity: Flagellar Motility and Germ-Soma Differentiation in Volvocalean Green Algae. *The American Naturalist* **167**, 537 (2006).
63. Koufopanou, V. The Evolution of Soma in the Volvocales. *The American Naturalist* 143, 907–931 (1994).
64. Leslie, M. P., Shelton, D. E. & Michod, R. E. Generation time and fitness tradeoffs during the evolution of multicellularity. *Journal of Theoretical Biology* **430,** 92–102 (2017).
65. Butterfield, N. J. Modes of pre-Ediacaran multicellularity. *Precambrian Research* **173,** 201–211 (2009).
66. Chen, L., Xiao, S., Pang, K., Zhou, C. & Yuan, X. Cell differentiation and germ–soma separation in Ediacaran animal embryo-like fossils. *Nature* **516,** 238–241 (2014).
67. Strassmann, J. E., Zhu, Y. & Queller, D. C. Altruism and social cheating in the social amoeba Dictyostelium discoideum. *Nature* **408,** 965–967 (2000).
68. Kuzdzal-Fick, J. J., Fox, S. A., Strassmann, J. E. & Queller, D. C. High Relatedness Is Necessary and Sufficient to Maintain Multicellularity in Dictyostelium. *Science* **334,** 1548–1551 (2011).
69. Kawecki, T. J. *et al.* Experimental evolution. *Trends in Ecology & Evolution* **27,** 547–560 (2012).
70. Meffert, L. M. & Bryant, E. H. Mating Propensity and Courtship Behavior in Serially Bottlenecked Lines of the Housefly. *Evolution* **45,** 293 (1991).
71. Wade, M. J. An Experimental Study of Kin Selection. *Evolution* **34,** 844 (1980).
72. Rainey, P. B. & Travisano, M. Adaptive radiation in a heterogeneous environment. *Nature* **394,** 69–72 (1998).

73. Herron, M. D., Hackett, J. D., Aylward, F. O. & Michod, R. E. Triassic origin and early radiation of multicellular volvocine algae. *Proceedings of the National Academy of Sciences* **106,** 3254–3258 (2009).
74. Khan, A. I., Dinh, D. M., Schneider, D., Lenski, R. E. & Cooper, T. F. Negative Epistasis Between Beneficial Mutations in an Evolving Bacterial Population. *Science* **332,** 1193–1196 (2011).
75. Fitzpatrick, M. J., Feder, E., Rowe, L. & Sokolowski, M. B. Maintaining a behaviour polymorphism by frequency-dependent selection on a single gene. *Nature* **447,** 210–212 (2007).
76. Becks, L. & Agrawal, A. F. Higher rates of sex evolve in spatially heterogeneous environments. *Nature* **468,** 89–92 (2010).
77. Taylor, D. R., Zeyl, C. & Cooke, E. Conflicting levels of selection in the accumulation of mitochondrial defects in *Saccharomyces cerevisiae*. *Proceedings of the National Academy of Sciences* **99,** 3690–3694 (2002).
78. Reboud, X. & Bell, G. Experimental evolution in Chlamydomonas. III. Evolution of specialist and generalist types in environments that vary in space and time. *Heredity* **78,** 507–514 (1997).
79. Wielgoss, S. *et al.* Mutation Rate Inferred From Synonymous Substitutions in a Long-Term Evolution Experiment With Escherichia coli. *G3: Genes|Genomes|Genetics* **1,** 183–186 (2011).
80. Gerstein, A. C., Chun, H.-J. E., Grant, A. & Otto, S. P. Genomic Convergence toward Diploidy in Saccharomyces cerevisiae. *PLoS Genetics* **2,** (2006).
81. Holloway, A. K., Palzkill, T. & Bull, J. J. Experimental Evolution of Gene Duplicates in a Bacterial Plasmid Model. *Journal of Molecular Evolution* **64,** 215–222 (2007).
82. Malmberg, R.L. Evolution of epistasis and advantage of recombination in populations of bacteriophage T4. *Genetics* **86,** 607–621 (1977).
83. Chao, L. et al. Muller's ratchet and the advantage of sex in the RNA virus φ6. Evolution **46,** 289–299 (1992).
84. Rebolleda-Gómez, M., Ratcliff, W. & Travisano, M. Adaptation and Divergence during Experimental Evolution of Multicellular Saccharomyces cerevisiae. *Artificial Life 13* (2012). doi:10.7551/978-0-262-31050-5-ch014
85. Ratcliff, W. C., Pentz, J. T. & Travisano, M. Tempo And Mode Of Multicellular Adaptation In Experimentally Evolved *Saccharomyces cerevisiae*. *Evolution* **67,** 1573–1581 (2013).
86. Dutcher, S. K. *et al.* Whole-Genome Sequencing to Identify Mutants and Polymorphisms in Chlamydomonas reinhardtii. *G3: Genes, Genomes, Genetics* 2, 15–22 (2012).
87. Lenski, R. E., Rose, M. R., Simpson, S. C. & Tadler, S. C. Long-Term Experimental Evolution in Escherichia coli. I. Adaptation and Divergence During 2,000 Generations. *The American Naturalist* **138,** 1315–1341 (1991).
88. Herron, M. D., Ghimire, S., Vinikoor, C. R. & Michod, R. E. Fitness trade-offs and developmental constraints in the evolution of soma: An experimental study in a volvocine alga. *Evol. Ecol. Res.* **16**, 203–221 (2014).
89. Willensdorfer, M. On the Evolution of Differentiated Multicellularity. *BioRxiv*. (2008).

90. Hanikenne, M. Chlamydomonas reinhardtii as a eukaryotic photosynthetic model for studies of heavy metal homeostasis and tolerance. *New Phytologist* **159,** 331–340 (2003).